Quaternary Research **58**, 62–72 (2002)
doi:10.1006/qres.2002.2357

Lake Level and Climate Changes between 42,000 and 18,000 ^{14}C yr B.P. in the Tengger Desert, Northwestern China

Hucai Zhang[1]

National Laboratory of Western China's Environmental Systems, MOE, Lanzhou University, Lanzhou, China; and Institut D'astronomie et de Géophysique G. Lemaître, Université Catholique de Louvain, 2 Chemin du Cyclotron, B-1348 Louvain-La-Neuve, Belgique

E-mail: zhang@astr.ucl.ac.be or hucaizhang@yahoo.com

Bernd Wünnemann

Geolab, Institute of Geographical Sciences, Free University of Berlin, Malteser Strasse 74-100, 12249, Berlin, Germany

Yuzhen Ma

National Laboratory of Western China's Environmental Systems, MOE, Lanzhou University, Lanzhou, China

Jinlan Peng

Nanjing Institute of Geology and Palentology, Academia Sinica, Nanjing 210008, China

Hans-J. Pachur

Geolab, Institute of Geographical Sciences, Free University of Berlin, Malteser Strasse 74-100, 12249, Berlin, Germany

Jijun Li, Yuan Qi, Guangjie Chen, and Hongbing Fang

National Laboratory of Western China's Environmental Systems, MOE, Lanzhou University, Lanzhou, China

and

Zhaodong Feng

National Laboratory of Western China's Environmental Systems, MOE, Lanzhou University, Lanzhou, China; and Department of Earth and Environmental Sciences, Montclair State University, Upper Montclair, New Jersey 07043

Received August 3, 2000

Multiple lines of stratigraphic, geochemical, and fossil data suggest that fresh-mesohaline paleolakes were widespread in the Tengger Desert of northwestern China and underwent major fluctuations during the late Pleistocene. The paleolakes started to develop at ca. 42,000 ^{14}C yr B.P. The lake levels were the highest between 35,000 and 22,000 ^{14}C yr B.P., during which Megalake Tengger dominated the landscape. The climatic conditions at this time were unique for this area and have no modern analogue. After an episode of decline between 22,000 and 20,000 ^{14}C yr B.P. and an episode of rebound between 20,000 and 18,600 ^{14}C yr B.P., the paleolakes started to desiccate and completely disappeared around 18,000 ^{14}C yr B.P. The environmental proxy data indicate that the Megalake Tengger formed under warm–humid climates. The reconstructed climatic variations appear to be correlative with the abrupt climatic events reconstructed for the North Atlantic.

Key Words: **Tengger Desert; climate change; lake levels.**

INTRODUCTION

Large-amplitude climatic instabilities at suborbital timescales that appear in the North Atlantic Ocean and adjoining areas (Heinrich, 1988; Johnson *et al.*, 1992; Bond *et al.*, 1993, 1995; Dansgaard *et al.*, 1993; Fronval *et al.*, 1995; GRIP members, 1995) have been used to suggest that the North Atlantic was a forcing center of these large-scale events (Broecker, 1995). Recently, however, the tropical Pacific Ocean has been assessed as an even more important forcing center (Cane, 1998; Clement and Cane, 1998; Sirocko *et al.*, 1999; Wang and Sarnthein, 1999; Leuschner and Sirocko, 2000). To understand the

[1] To whom correspondence should be addressed.

0033-5894/02 $35.00

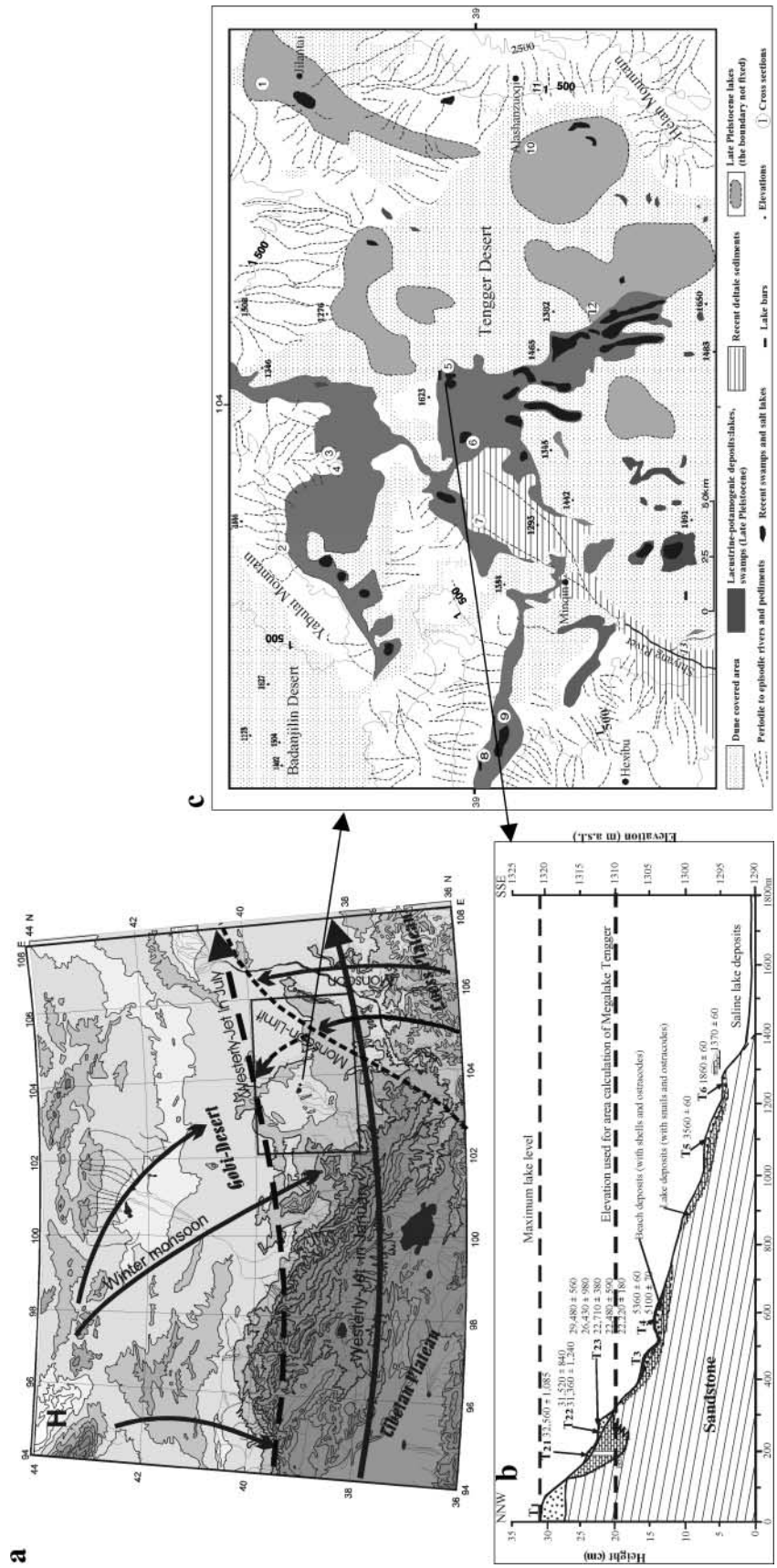

FIG. 1. Study area: a) Climatological and geomorphological settings. Dotted lines indicate the boundaries between Gobi-Desert, Tibetan Plateau, and Loess Plateau. b) Baijian Hu terraces (site 5 in Fig. 1c), ^{14}C dates, and estimated paleolake levels. c) Study sites and reconstructed scope of the Megalake Tengger.

geographic patterns and the teleconnection mechanisms of these well-documented climatic instabilities, regional records must be explored (Broecker, 1997). The Tengger Desert, at the junction of the Chinese Loess Plateau, the Tibetan Plateau, and the Mongolian Plateau deserves special attention in that regard, because the westerlies displaced by the Tibetan Plateau, high-latitude continental air masses, and low-latitude maritime air masses (summer monsoons) (Fig. 1a) all interacted in this area during the Quaternary (Li *et al.*, 1988; Prell and Kutzbach, 1987; Zhou, 1996; An *et al.*, 2001).

This study focuses on the Tengger Desert to reconstruct the sequences of paleoenvironmental events. The desert is bounded by the Qilian Mountains on the southwest and the Helan Mountain on the east. Yabulai Mountain demarcates its northwestern boundary, and the Loess Plateau touches its southeastern tip. Climatically, the area is transitional from the arid northwest, the semiarid southeast, and the cold mountainous southwest. Driven by warming of the plateaus and influenced by the meandering of the westerly jet stream, the East Asian Monsoon brings precipitation into the Tengger Desert during the summer. The cold, dry air masses associated with the Siberian–Mongolian high-pressure system generally prevail during the winter. The mean annual precipitation is 115 mm, the mean annual temperature is 7.8°C, and the potential annual evaporation is as high as 2600 mm (Agricultural Regional Commission, 1985). Today, there is no permanent lake in the Tengger Desert, although it is a closed hydrological system.

Our previous investigations (Zhang and Wünnemann, 1997; Wünnemann *et al.*, 1998; Zhang *et al.*, 2001b) identified six paleolake terraces (Fig. 1b) in the Baijian Hu area (39°09′N, 104°10′E), the center of the Tengger Desert. The highest terrace T_1 is 30–31 m above the present Baijian Hu playa surface and is not dated for lack of datable matter. The second terrace T_2, the Main Terrace, is ca. 22 m above the playa surface. T_2 can be divided into three parts: a broken terrace ($T_{2,1}$) on the outer side and two well-preserved parallel terraces ($T_{2,2}$ and $T_{2,3}$) on inner side. Terrace $T_{2,1}$ is dated at 32,560 ± 1,090 yr ^{14}C B.P. Dates for terrace $T_{2,2}$ are 31,520 ± 840 and 31,360 ± 1,240 ^{14}C yr B.P. Five dates on terrace $T_{2,3}$, range from 30,000 to 22,000 ^{14}C yr B.P. (29,480 ± 560, 26,430 ± 980, 22,710 ± 380, 22,480 ± 590, and 22,220 ± 180 ^{14}C yr B.P.). The other terraces are dated at 8450 ± 90 ^{14}C yr B.P. (T_3), 5360 ± 60 ^{14}C yr B.P. and 5100 ± 70 ^{14}C yr B.P. (T_4), 3560 ± 60 ^{14}C yr B.P. (T_5), and between 1860 ± 60 and 1370 ± 60 ^{14}C yr B.P. (T_6) and formed during the Holocene.

On the basis of the elevations of Baijian Hu terraces, and the distribution of lacustrine–fluvial deposits in the Yabulai Mountain area referred to the elevation of regional lake deposits recorded at 12 sites in the Tengger Desert (Fig. 1c), it was deduced that the high stand of Megalake Tengger during the Late Pleistocene was between 1310 and 1321 m above sea level. The paleolake area calculated along the 1310-m hypsometeric contour is 16,000 km^2 (Pachur *et al.*, 1995). It was later found that there are several separate paleolakes in the eastern part of the desert. Because this high stand is 2 m lower than the main beach (T_2) and 8–9 m lower than T_1, the recalculated total area of the paleolakes between 35,000 and 22,000 ^{14}C yr B.P. in the Tengger Desert should be at least 20,000 km^2 (Fig. 1c), more than half of the total area of the Tengger Desert (Zhang *et al.*, 2001a, 2001b).

Ostracode assemblages indicate that the paleolakes were fresh-mesohaline (Peng *et al.*, 1998), and the associated climate was warmer and moister than today (Zhang and Wünnemann, 1997; Ma *et al.*, 1998). These conclusions are further supported by investigations on a section between Yabulai Mountain and piedmont areas in the western Tengger Desert (Zhang *et al.*, 2001b). This "warmer and moister" paleoclimatic reconstruction for 35,000–22,000 ^{14}C yr B.P. from the Tengger Desert (i.e., the Megalake Tengger period) agrees with the climate reconstructed from the Guliya ice core in the Qiliang Mountains (Thompson *et al.*, 1997; Yao *et al.*, 1997) and seems consistent with reconstructions from other areas in northwestern China (Li *et al.*, 1991; Huang, 1994; Rhodes *et al.*, 1996; Li and Zhu, 2001). In this paper, we report our newly obtained high-resolution multiproxy data from Duantouliang (DTL) section in the Tengger Desert to improve the paleoclimatic reconstructions for the period 40,000–18,000 ^{14}C yr B.P. and further explore the climatic significance in the context of global change.

METHODS

Previous studies (Pachur *et al.*, 1995; Zhang and Wünnemann, 1997; Ma *et al.*, 1998; Peng *et al.*, 1998) focused on the DTL section (site 3, Fig. 1c) and provided a sketchy history of environmental change there. The details of the history need to be explored to address the temporal and spatial significance of the climatic instabilities mentioned above and inferred from elsewhere. For this purpose, we reexcavated the DTL section and also the Tudongcao (TDC) section (site 4) and described carefully both sections in the field for stratigraphic comparison. TDL was then sampled at intervals of 7–10 cm between depths of 0–34 cm and 360–400 cm, and at intervals of 2–5 cm for the rest of this 400-cm section. In all, 92 samples were obtained and analyzed for elemental composition using the inductively coupled plasma (ICP) technique. Standard methods were applied for pollen and ostracode identifications. Grain size was analyzed by a combination of elutriation and wet sieving (Allen, 1975). The chronology was based on eight ^{14}C dates of organic matter, reinforced by eight ^{14}C dates on organic matter from the nearby TDC section (Fig. 2) and ^{14}C dates from the Baijian Hu beach–terrace sequence. In addition, one ^{14}C date on fossil shells (*Corbicula fluminea müller* and *Corbicula lorgillierti philippi*) from the DTL section that fits the chronological framework of the other dates seems acceptable because the shells consist only of aragonite, with no recrystallization to calcite, and therefore no carbonate exchange between the shell and ground water. Furthermore, because there are no carbonate rocks in the area and the water of paleolake Tengger was fresh-mesohaline, as

indicated by the ostracode assemblages (Peng *et al.*, 1998), the hard-water reservoir effect was limited. ^{14}C dating was done at Lanzhou University and Lanzhou Desert Institute of China (conventional), at the Bundesanstalt für Geowissenchaften und Rohstoffe in Hannover, Germany (both conventional and accelerator mass spectroscopy [AMS]), and at Beta Analytic, Miami, USA (AMS). A half-life of 5568 yr was applied and the ages were not calibrated. The ages between any pair of radiocarbon dates were calculated by linear interpolation.

STRATIGRAPHY AND CHRONOLOGY

The 400-cm DTL section can be divided into six stratigraphic units, as shown in Figure 2. Unit 1 (0–34 cm) consists of well-sorted carbonate-cemented beach gravel interbedded with silty clay deposits containing fossil shell fragments.

Unit 2 (34–80 cm) consists of light brown to slightly gray-green clayey fine sand and gravel, cemented by carbonate and enriched in fossil snail fragments. The two dated samples were from depths of 34–40 cm (18,860 ± 340 ^{14}C yr B.P.) and 75–80 cm (20,060 ± 410 ^{14}C yr B.P.).

Unit 3 (80–150 cm) consists of sand and gravel enriched in fossil shell fragments. The unit can be divided into five subunits. From 80 to 113 cm is a well-sorted, un-cemented beach-gravel layer containing numerous fossil shell fragments; from 113 to 118 cm is a layer of fossil shells (*Corbicula fluminea müller* and *Corbicula lorgillierti philippi*), dated at 21,150 ± 420 ^{14}C yr B.P.; from 118 to 125 cm is a sandy gravel layer cemented by carbonates; from 125 to 135 cm is a well-sorted, uncemented beach gravel; and from 135 to 150 cm is sand.

Unit 4 (150–322 cm) consists mainly of lacustrine deposits with fragments of freshwater snails. This unit can be divided into 11 subunits (designated as a–k). Unit 4a, from 150 to 175 cm, is clayey-silt in the upper part and silty-clay in the lower part. The lower part contains fossil snails. A sample from 170–175 cm was dated at 22,950 ± 530 ^{14}C yr B.P. Unit 4b, 175–180 cm, is silty sand containing fragments of fossil shells; Unit 4c, from 180 to 211 cm, contains brown-yellowish silty-clay layers interbedded

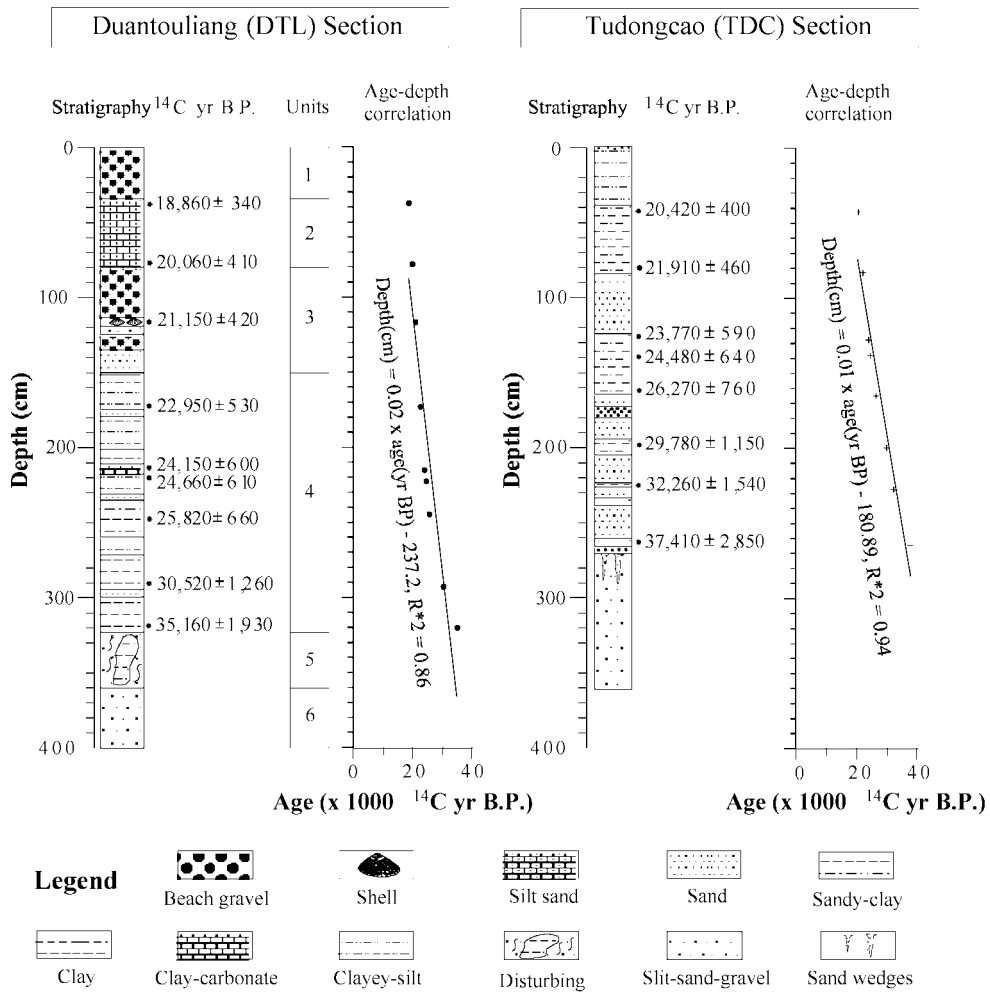

FIG. 2. Stratigraphy and age-depth relation of Duantouliang (DTL) section, with the reference to the age-depth relation of the nearby Tudongcao (TDC) section.

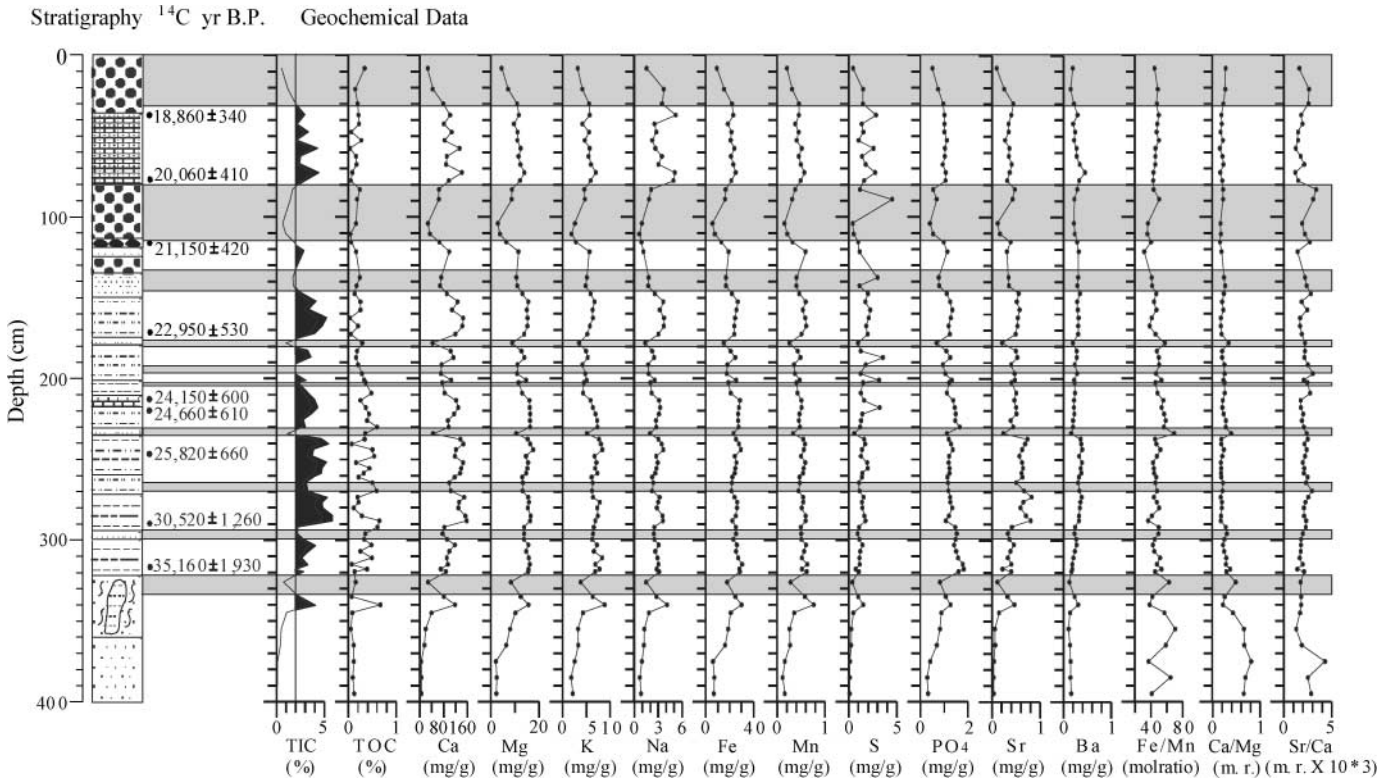

FIG. 3. Stratigraphy and geochemical results of Duantouliang (DTL) section. The highlighted intervals are the time periods when both TIC contents and lake levels were low. m. r. = mol ratio. Legends for the stratigraphy are the same as in Figure 2.

with fine silt layers from 180 to 190 cm, and grayish fine silt layers interbedded with grayish clay layers from 190 to 200 cm. From 200 to 202 cm is a marker layer of brownish, silty clay. From 202 to 211 cm is a grayish silt layer interbeded with grayish clay layer containing fossil snails. Unit 4d, from 211 to 217 cm, is a bedded clay layer enriched in carbonate and fossil shells and snails. It was dated at 24,150 ± 600 ^{14}C yr B.P. Unit 4e, from 217 to 232 cm, contains clay layers interbedded with fine silt layers enriched in fossil snails. A sample at the depth 220–224 cm was dated at 24,660 ± 610 ^{14}C yr B.P. Unit 4f, from 232 to 236 cm, is a brown-yellowish sand layer. Unit 4g, from 236 to 260 cm, consists of grayish clay layers interbedded with grayish fine silt layers. A sample at 242–246 cm was dated at 25,820 ± 660 ^{14}C yr B.P. Unit 4h, from 260 to 272 cm, is a silt layer. Unit 4i, from 272 to 294 cm, is a grayish clay layer containing fragments of fossil snails. A sample from the 290–294 cm was dated at 30,520 ± 1,260 ^{14}C yr B.P. Unit 4j, from 294 to 298 cm, is a light brownish fine silt layer with fossil snails. Unit 4k, from 298 to 322 cm, is a bedded clay layer with fossil snails. A sample from 317–322 cm was dated at 35,160 ± 1,930 ^{14}C yr B.P.

Unit 5 (322–360 cm) is a disturbed and mixed layer of red-brown silt-sand-gravel deposits capped with a thin yellow-brownish clay layer.

Unit 6 (360–400 cm) consists of brown-red silt-sand-gravel deposits. This layer is widely distributed in the area and thus regarded as a regional stratigraphic marker.

On the basis of the regional stratigraphical and chronological correlations (Zhang *et al.*, 2001b) and age extrapolation, the bottom of the section appears to have formed between 42,000 and 40,000 ^{14}C yr B.P. The nearly linear relationship between dates and depths reinforced our confidence in the ^{14}C dates and reduced the possibility that there was a depositional hiatus in the section.

ELEMENTAL GEOCHEMISTRY

Elemental concentrations for the DTL section are summarized in Table 1. They show that the geochemical composition varies

TABLE 1
Concentration Ranges for Different Elements in the Duantouliang Section

TOC (%)	TIC (%)	Ca (mg/g)	Mg (mg/g)	Sr (mg/g)	Ba (mg/g)
0.03–0.65 (0.25)	0.06–4.77 (2.55)	4.03–157.23 (91.21)	1.98–17.57 (12.26)	0.03–0.83 (0.41)	0.10–0.49 (0.26)
Fe (mg/g)	**Mn (mg/g)**	**K (mg/g)**	**Na (mg/g)**	**S (mg/g)**	**P(PO_4) (mg/g)**
5.60–29.93 (21.69)	0.15–0.77 (0.46)	1.80–8.81 (5.63)	0.62–5.18 (2.58)	0.08–4.52 (1.42)	0.29–1.81 (1.11)

Note. Data in parentheses are the average values. TOC, total organic carbon; TIC, total inorganic carbon.

widely, affording an opportunity to distinguish the depositional environments. The relationship between total inorganic carbon (TIC) and lithology, shown in Figure 3, suggests that the TIC content is a good indicator of the depositional environment. For example, the TIC values are lower than 2% for typical sand layers, around 2% for beach sediments, and higher than 2% for lacustrine deposits. The stratigraphic characteristics of lacustrine deposits and corresponding TIC values indicate that the higher the TIC values, the higher the lake levels were. Three elements, Ca, Sr, and Mg, closely covary with the TIC (Fig. 4) are used as indices for water depth and water pH (Zhang, 1997). As an index of oxidation, the Fe/Mn ratio is indirectly related to water depth (Hakanson and Jansson, 1983). The total organic carbon (TOC) as an index of organic productivity, and the Ca/Mg ratio as an index of aridity, are both affected by the effective soil moisture, which in turn is controlled by both the precipitation and temperature. The photosynthetic activity indicator, Mg (Gasse *et al.*, 1991), and a water salinity indicator, the Sr/Ba ratio, are closely correlated, as expected, in this salt-constrained ecological environment. These environmental proxies are considered to be useful in the arid areas of northwestern China (Gasse *et al.*, 1996; Zhang *et al.*, 2000) and have been tested there with satisfactory results (Qi, 1999, unpublished data).

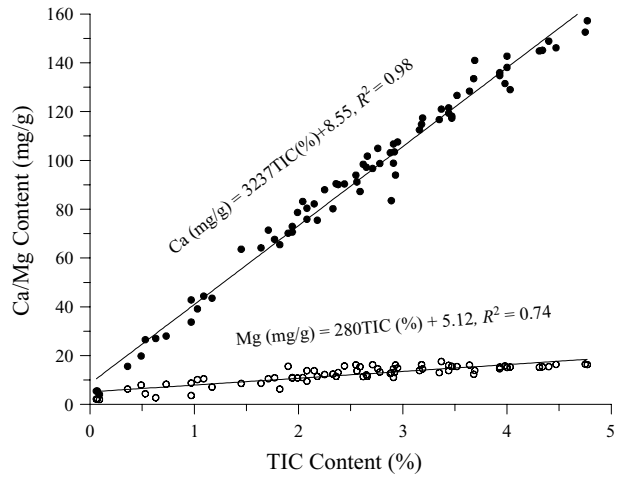

FIG. 4. Correlations between total inorganic carbon (TIC) and Ca and Mg concentrations at the Duantouliang (DTL) section.

GRAIN SIZE

Seven fractions of grain sizes were separated: >0.4 mm, 0.4–0.1 mm, 0.1–0.075 mm, 0.075–0.05 mm, 0.05–0.01 mm, 0.01–0.005 mm, and <0.005 mm (Fig. 5). An additional two

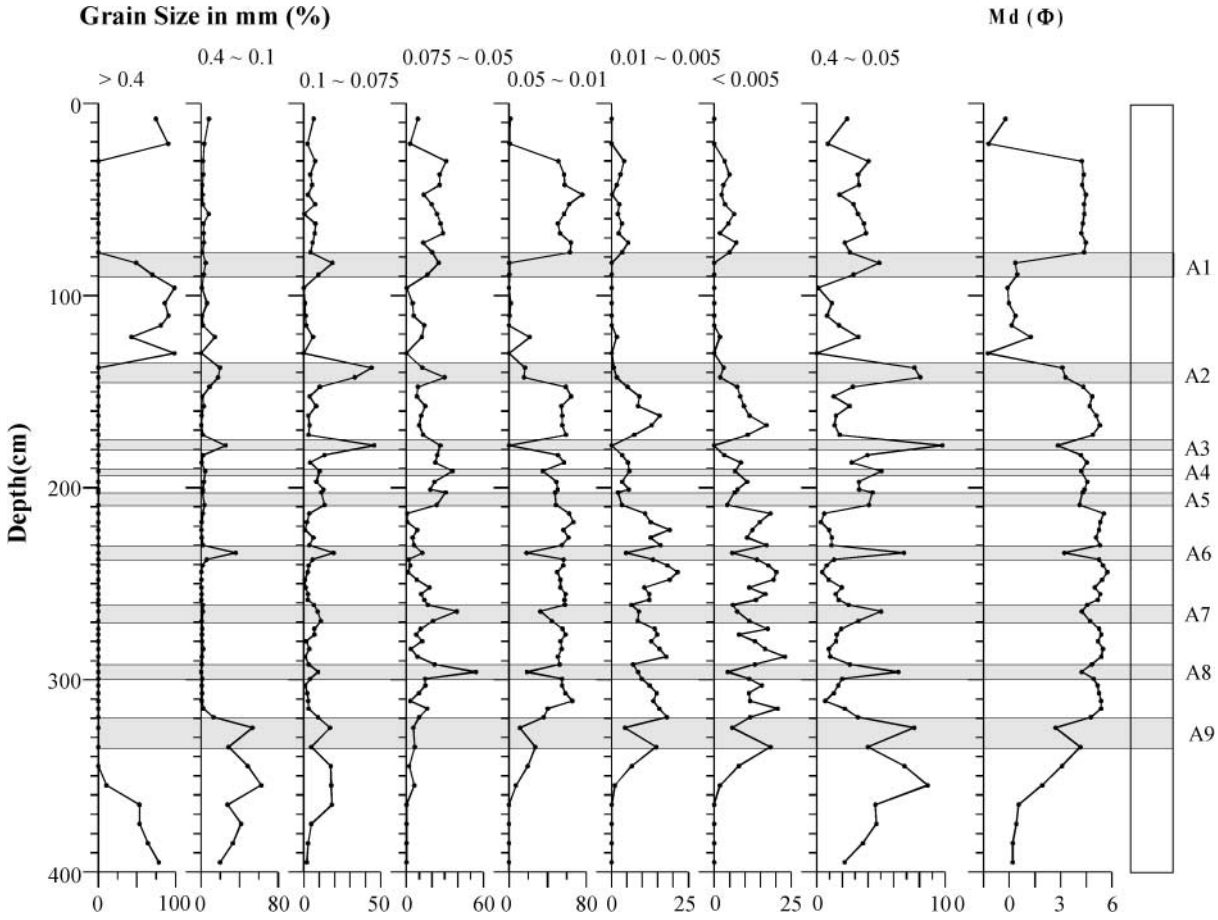

FIG. 5. Grain-size variations at Duantouliang (DTL) section. A1-9 mark nine peaks of eolian component (0.4–0.05 mm fraction).

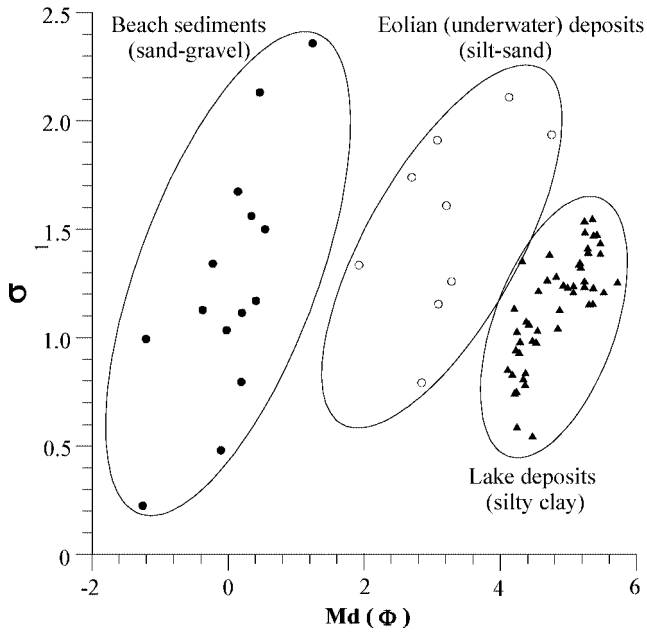

FIG. 6. Depositional phases and δ-M_d dispersion of grain size at the Duantouliang (DTL) section.

fractions, >1.25 mm and 1.25–1.00 mm, were separated in layers containing coarse sand. On the basis of depositional phase analyses and δ-M_d dispersion (Ren and Wang, 1980), the fractions were divided into three groups representing three depositional phases: >0.4 mm, the beach deposit; 0.4–0.05 mm, sand and/or eolian accumulation; and <0.05 mm, lake (with airborne) deposits (Fig. 6).

Typical beach depositional properties (see Fig. 6) are clearly exhibited in the strata at depths of 0–34 cm and 80–137 cm in the DTL section. The inferred beach environment for these two strata is also supported by the shallow freshwater species of shells (*Corbicula fluminea Müller* and *Cubicula Largillierti philippi*) and snails (*Gyraulus chinensis*). Fine sand is a major component of the eolian (surface wind) deposits. An increase in 0.4–0.05 mm fraction can be interpreted as indicating of sanddune activation, expansion of desert, and/or strengthening of wind (Porter and An, 1995; Xiao *et al.*, 1995). Nine peaks of the 0.4–0.05 mm fraction in the stratigraphic column (A1–A9 in Fig. 5) suggest that eolian activities strengthened nine times, probably under drying climates during the studied period (42,000–18,000 ^{14}C yr B.P.). During periods of high lake levels, the depositional environments were stable and the deposits are basically composed of silty-clay to clayey-silt with the average grain size ranging between 0.03 and 0.05 mm.

POLLEN AND OSTRACODES

Four major pollen zones were identified on the basis of palynomorphs and pollen concentrations. These zones are labeled from the top to the bottom as 4, 3, 2, and 1 in Figure 7. Ages for each sample were interpolated or extrapolated from the dates from DTL section. Zone 4, from the surface to 39.7 cm in the DTL section, dates to ca. 18,050–19,010 ^{14}C yr B.P. Pollen concentration in Zone 4 is the highest in the entire DTL section. *Artemisia* is from 14.6% to ~64.3% (average: 55.4%) of the total pollen, and *Nitraria* is up to 29.3% (average: 11.6%). The pollen concentration of *Picea, Betula*, and *Salix* increased

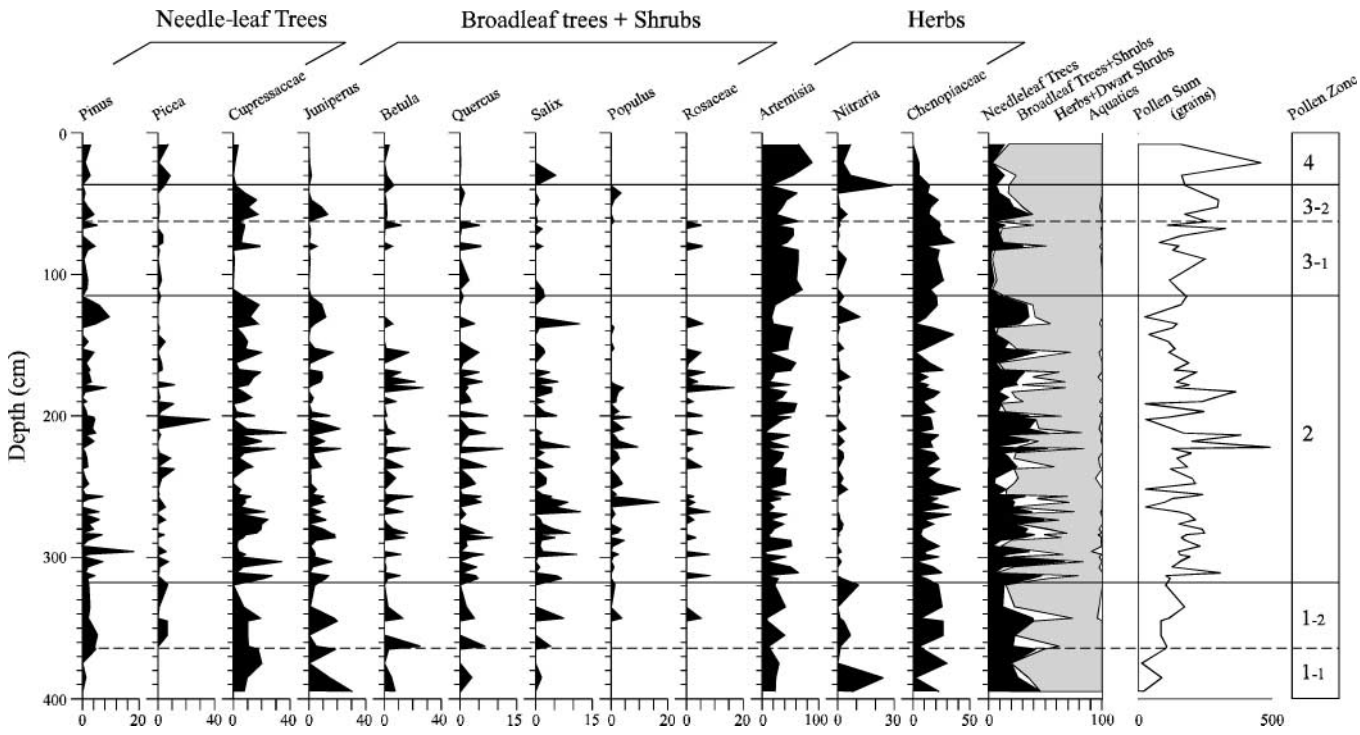

FIG. 7. Major pollen assemblages and pollen zones of the Duantouliang (DTL) section.

TABLE 2
Statistical Data for Ostracodes in the Duantouliang Section (Valves/20 g Sample)

No.	Depth (cm)	Limnocythere inopinata	Darwinula stevensoni	Candona neglecta	Cyprideis torosa	Ilyocypris gibba	Cyclocypris serena	?Neocypridopsis sp.
N11t	73.5	6544	1560	168	144	0	8	0
N11s	111	393	202	16	5	1	0	0
N11r	137.5	3808	3248	1176	216	88	24	0
N11q	152.5	99	29	1	0	0	0	0
N11p	167.5	225	98	4	0	2	0	0
N11o	177	291	525	55	14	3	0	0
N11n	182	986	354	19	1	1	0	0
N11l	193	5200	6624	208	16	8	0	0
N11m	201.5	470	378	22	2	0	0	0
N11k	214	76	39	6	0	0	0	0
N11j	223.5	72	1	0	0	0	0	0
N11i	236.5	86	2	0	0	0	0	0
N11h	256.5	174	20	0	2	0	0	0
N11g	267.5	190	2	1	0	0	0	0
N11f	282.5	125	7	3	0	0	0	0
N11e	287.5	56	4	2	0	0	0	0
N11d	297.5	38	4	3	1	0	0	0
N11c	312.5	72	10	0	1	0	0	0
N11b	345	35	0	4	2	0	0	2
N11a	365	0	0	0	0	0	0	0

compared to the underlying Zone 3, while *Chenopodiacea* decreased. *Quercus, Populus*, and *Rosaceae* are absent in Zone 4.

Zone 3, from 39.7 to 118.5 cm, dates to ca. 19,010–21,260 ^{14}C yr B.P. Pollen concentration in Zone 3 is also high, but the percentages for both needle-leaf and broadleaf trees are lower than in the underlying Zone 2 and the number of species, especially the taxa of broadleaf trees and shrubs, are also reduced relative to Zone 2. For instance, *Populus* is absent and *Betula, Quercus, Salix*, and *Rosaceae* are rare. The herbs, such as *Artemisia* and *Chenopodiaceae*, dominate the pollen spectra. Variations in *Cupressaseae, Juniperus, Populus*, and *Rosaceae* divide Zone 3 into two subzones: 3_2 (upper portion) and 3_1 (lower portion). The division is at the depth of 78.7 cm, corresponding to ca. 20,160 ^{14}C yr B.P.

Zone 2, from 118.5 to 317.2 cm, dates to ca. 21,260–34,660 ^{14}C yr B.P. Pollen concentration in this zone is generally high, and the number of species is the highest in the entire DTL section. All of the representative taxa, such as needle-leaf trees (*Pinus, Piceae, Cupressaseae*, and *Juniperus*), broadleaf trees and shrubs (*Betula, Quercus, Salix, Populus*, and *Rosaceae*), and herbs (*Artemisia, Nitraria*, and *Chenopodiacea*), vary drastically in terms of frequency (occurrence) and magnitude (percentage). The percentages of both needle-leaf and broadleaf tree pollen increased, and the percentage of *Nitraria* pollen decreased, relative to Zone 1.

Zone 1, from 317.2 to 400 cm, dated to ca. 34,660–40,500 ^{14}C yr B.P. Pollen concentration is generally low. The most abundant taxa are *Cupressaseae, Juniperus, Nitraria,* and *Chenopodiacea*. Needle-leaf tree pollen accounts for 12.4% to ~46.2% of the total, and the percentage of broadleaf tree pollen is low. Zone 1 can be divided at 364 cm (ca. 38,290 ^{14}C yr B.P.) into Zone 1_2 (upper portion) and Zone 1_1 (lower portion) on the basis of the sudden appearance in the record of needle-leaf trees such as *Pinus* and *Picea* and broadleaf trees such as *Betula, Quercus, Salix, Populus, Rosaceae*, and others.

Macrofossil identification shows that seven species of ostracodes (*Limnocythere inopinata, Darinula stevensoni, Candona neglecta, Cyprideis torosa, Ilyocypris gibba, Cyclocypris serenna*, and *Neocypridopsis* sp.) from the DTL section lived in a fresh-mesohaline lake during the Megalake Tengger period (35,000–22,000 ^{14}C yr B.P.) (Peng *et al.*, 1998; Table 2). This finding is in agreement with the environmental interpretation from geochemical indices such as Ca/Mg and Sr/Ca ratios, and elemental concentrations of S and Na (see Fig. 3).

DISCUSSION AND CONCLUSION

The history of climatic change in the Tengger Desert can be reconstructed on the basis of the proxies from the DTL section. In the bottom portion of the section, at depths of 400–360 cm (ca. 42,000 to ~38,000 ^{14}C yr B.P.) in pollen subzone 1_1, TIC, TOC, Ca, Mg, S, and Na are all low, and the pollen spectrum is dominated by *Artemisia, Chenopodiacea* and *Cupressaceae, Juniperus*, and *Gramineae*. The climate during this period inferred from the pollen spectra was dry, but the low concentrations of soluble elements and the red-brownish deposits which are different from the deposits of other parts in the section suggest that the effective soil moisture might have been relatively high.

From 360 to 322 cm (38,000 to 35,390 ^{14}C yr B.P.), the DTL section contains a mixture of the overlying lacustrine deposits

and the underlying playa sediments. This layer corresponds to the pollen subzone 1_2 and represents a cooling of the climate, leading to an increase in the content of *Picea* and a decrease in the total pollen. In the nearby TDC section, sandy wedges were found in the playa layer, and the overlying deposit was dated at 37,410 ± 2,850 ^{14}C yr B.P. The sandy wedges indicated a period of cold. Permafrost activity formed the sandy wedges at the TDC site and disturbed the strata at the DTL site, from ca. 38,000 to 35,390 ^{14}C yr B.P.

From 322 to 113 cm (35,390 to 21,070 ^{14}C yr B.P.), corresponding to the pollen zone 2, is the main phase of the Megalake Tengger. TOC, TIC, Ca, Mg, and Sr are all generally high, but there were abrupt decreases at 31,490–30,330 ^{14}C yr B.P., 25,390–25,190 ^{14}C yr B.P., and 23,260–23,030 ^{14}C yr B.P. The high-frequency, large-amplitude oscillations of lake levels and pollen assemblages indicate climatic instabilities during this period.

From 113 to 80 cm (2070 to 20,140 ^{14}C yr B.P.), corresponding to pollen zone 3_1, the TIC content decreased. The lake level lowered so much that the area where DTL and TDC sections are located became a beach. Herbs (e.g., *Artemisia, Chenopidiaceae, Graminea)* and some needle-leaf trees (e.g., *Cupreseaceae*) dominated the pollen spectra. From 80 to 34 cm (20,140 to 18,760 ^{14}C yr B.P.), corresponding to the pollen zone 3_2, increases in TIC and related chemical elements suggest that the lake level rose again. After 18,760 ^{14}C yr B.P. (pollen zone 1), the lake level declined again, and a new beach environment formed. This was sustained until ca. 18,000 yr B.P., when the paleolakes disappeared completely from the Tengger Desert.

The climate changes indicated by the pollen and stratigraphic records appear to be out of phase (Zhang *et al.*, 2000b). For example, permafrost conditions ended at 35,390 ^{14}C yr B.P., but the pollen-indicated warmer and more humid conditions did not begin until ca. 34,660 ^{14}C yr B.P., about 730 yr later. The stratigraphy suggests a lake-level decline at 21,260 ^{14}C yr B.P., but this was followed by vegetation changes associated with climatic deterioration at ca. 21,070 ^{14}C yr B.P., 190 yr later. The lag between the indicators may simply imply that vegetation communities, especially forests, have a kind of inertia and take longer to become established following the onset of favorable climatic conditions than the ecosystem takes to respond to climatic deterioration.

In the DTL section, low pollen concentrations of both needle-leaf and broadleaf trees coincide with low total pollen sums. Peaks of the 0.4–0.05 mm grain-size fractions for the same intervals imply heightened eolian deposition then (A1–A9 in Fig. 5), and low water levels are indicated by TIC and related elements (Fig. 3). This complex suggests cold–dry climatic conditions. The cold climatic events documented by the peaks of grain size 0.4–0.05 mm appear to correlate with the Heinrich events (Heinrich, 1988; Bond and Lotti, 1995). For instance, grain-size peak A_2 may correlate with Heinrich event H2, A_7 to H3 and A_9 to H4 (Fig. 8). This correlation, although tentative and

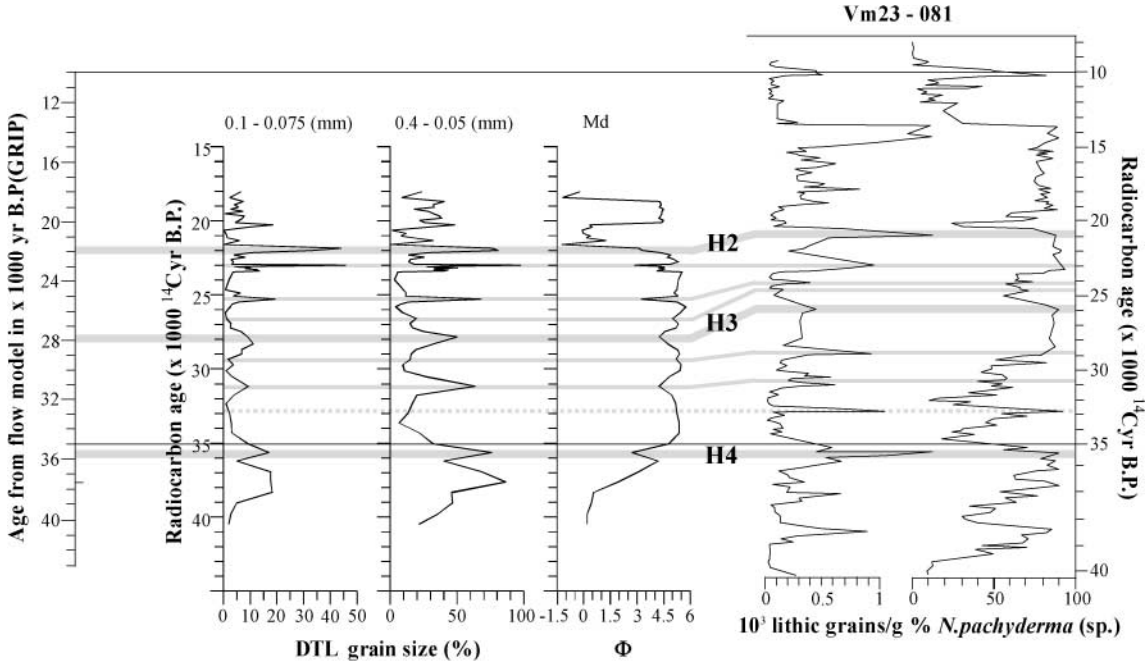

FIG. 8. Correlation between Heinrich events recorded in Tengger Desert and deep-sea sediments (Bond and Lotti, 1995). In this correlation, the peaks match each other well (thick shaded lines). Limited by the resolution of grain size data between H4 and H3 in the Duantouliang (DTL) section, there is one more peak in the deep-sea sediments than in the DTL section (dashed shaded line). There appear to be many differences in the geological records from this period (see Thomson *et al*., 1995; Rasmussen *et al*., 1997; Veiga-Pires and Hillarie-Marcel, 1999). Because our results match the ages of Heinrich events in the GRIP chronology, we argue that the correlation is meaningful. Two lines mark reference ages of 35,000 and 10,000 yr B.P. in the scale of GRIP, DTL, and Vm23-081.

qualitative, may support the teleconnection between the North Atlantic Ocean and the Chinese Loess Plateau hypothesized by Porter and An (1995) on the basis of the distribution of eolian quartz grains.

In summary, the Megalake Tengger formed between 35,000 and 22,000 ^{14}C yr B.P. under climatic conditions that have no modern analogues and were unique during the late Pleistocene (Zhang *et al.*, 2000). The "Greatest Lake Period" that occurred on the Tibetan Plateau from 40,000 to 25,000 ^{14}C yr B.P. (Li and Zhu, 2001), the multiple soil-forming events in the northern Mongolian Plateau from approximately 40,000 to 22,000 ^{14}C yr B.P. (Feng, 2001), and the reducing-dominated environment in the western Chinese Loess Plateau from approximately 40,000 to 20,000 ^{14}C yr B.P. (Feng *et al.*, 1998) all raise an interesting question: why does orbital forcing not appear to have been the prime factor controlling the climate in east-central Asia during marine isotope stage 3?

ACKNOWLEDGMENTS

This research was supported by the NSFC (no. 49971015 and 49731010) and the Education Committee Scientific Research Found to Zhang. It also has been included in and supported by the DFG in the framework of the cooperation between FU Berlin and Lanzhou University. A recent grant (A 973 project: on Desertification Processes and Prevention Methods in Northern China) from the Chinese Department of Science and Technology (grant no. G2000048701) also supported this study. Special thanks to D. Williams and an anonymous reviewer for their valuable suggestions and comments, which improved the paper.

REFERENCES

Agricultural Regional Commission. (1985). Agricultural Report of Minqin County, Gansu Province. Gansu Provincial Publishing House. [in Chinese]

Allen, T. (1975). "Particle Size Measurement," 2nd ed. (pp. 121–122). Chapman and Hall, New York.

An, Z. S., Kutzbach, J. E., Prell. W. L., and Porter, S. C. (2001). Evolution of Asian monsoon and phased uplift of the Himalayas-Tibetan plateau since late Miocene times. *Nature* **411,** 62–66.

Bond, G. C., and Lotti, R. (1995). Iceberg discharges into the North Atlantic on Millennial time scales during the Last Glaciation. *Science* **267,** 1005–1010.

Bond, G. C., Broecker, W. S., Johnsen, S., McManus, J., Labeyrie, L., Jouzel, J., and Bonani, G. (1993). Correlations between climate records from the North Atlantic sediments and Greenland ice. *Nature* **365,** 143–147.

Broecker, W. S. (1995). Massive iceberg discharge as triggers for global climate change. *Nature* **372,** 421–424.

Broecker, W. S. (1997). Future directions of Paleoclimate research. *Quaternary Science Reviews* **16,** 821–825.

Cane, M. A. (1998). A role for the Tropical Pacific. *Science* **282,** 59–61.

Clement, A., and Cane, M. A. (1998). A role for the Tropical Pacific coupled Ocean-Atmosphere System on Milankovitch millennial timescales. Part I: A modeling study of Tropical Pacific variability. *In* "Mechanisms of Global Climate Variability at Millennial Timescales" (P. U. Clarke, R. S. Webb, and L. D. Keigwin, Eds.), pp. 243–262. *American Geophysical Union Monograph* **112**.

Dansgaard, W., Johnson, S. J., Clausen, H. B., Dahjiensen, D., Gundestrup, N. S., Hammer, C. U., Hvidberg, C.S., Steffensen, J. P., Sveinbjorndottir, A. E., Jouzel, J., and Bond, G. (1993). Evidence for general instability of past climate from a 250-kya ice core record. *Nature* **364,** 218–220.

Feng, Z.-D. (2001). Gobi dynamics in the northern Mongolian Plateau during the past 20,000+ yr: preliminary results. *Quaternary International* **76/77,** 77–83.

Feng, Z.-D., Chen, F.-H., Tang, L.-Y., and Kang, J.-C. (1998) East Asian monsoon variations and Gobi dynamics during MIS 3 and 4. *Catena* **33,** 29–46.

Fronval, T., Jansen, E., Bloemendal, J., and Johnson, S. (1995). Oceanic evidence for coherent fluctuations in Fennoscandian and Laurentide ice sheets on millennium timescales. *Nature* **376,** 443–446.

Gasse, F., Arnold, M., Fontes, J.-Ch., Fort, M., Huc, A., Li, B., Liu, Q., Melieres, F., Van Campo, E., Wang, F., and Zhang, Q. (1991). A 13,000 year climate record from western Tibet. *Nature* **353,** 742–745.

Gasse, F., Fontes, J.-Ch., Van Campo, E., and Wei, K. (1996). Holocene environmental changes in Bangong Co basin (western Tibet). Part 4. Discussion and conclusions. *Palaeogeography, Palaeoclimatology, Palaeoecology* **120,** 79–92.

GRIP Members. (1995). Climate instability during the last interglacial period recorded in the GRIP ice core. *Nature* **364,** 203–207.

Hakanson, L., and Jansson, M. (Eds.). (1983). "Principle of the Lake Sedimentology," pp. 95–117. Springer-Verlag, Berlin.

Heinrich, H. (1988). Origin and consequences of cyclic ice rafting in the Northeast Atlantic Ocean during the past 130,000 years. *Quaternary Research* **29,** 142–152.

Huang, W. W. (1994). The prehistoric human occupation of the Qinghai-Xizang Plateau. *Göttinger Geographische Abhandlungen, Heft* **95,** 201–219.

Johnson, S. J., Clausen, H. B., Dansgaard, W., Fuhrer, K., Gunstrup, N., Hammer, C. U., Iversen, P., Jouzel, J., Stauffer, B., and Steffensen, J. P. (1992). Irregular glacial interstadials recorded in a new Greenland ice core. *Nature* **359,** 311–313.

Leuschner, D. C., and Sirocko, F. (2000). The low-latitude monsoon climate during Dansgaad-Oeschger cycles and Heinrich Events. *Quaternary International* **19,** 243–254.

Li, B. Y., and Zhu, L. P. (2001). "Greatest lake period" and its palaeoenvironment on the Tibetan Plateau. *Journal of Geographical Sciences* **11,** 34–42.

Li, B. Y., Zhang, Q. S., and Wang, F. B. (1991). Lake evolution history in Karakulun-West Kunlun Mountains. *Quaternary Sciences* **1,** 64–71.

Li, J. J., Feng, Z.-D., and Tang, L. Y. (1988). Late Quaternary monsoon patterns on the Loess Plateau of China. *Earth Surface Processes and Landforms* **13,** 125–135.

Ma, Y. Z., Zhang, H. C., Li, J. J., Pachur, H.-J., and Wünnemann, B. (1998). On the evolution of the palynoflora and climatic environment during Late Pleistocene in Tengger Desert. *Acta Botanica Sinica* **40,** 871–879.

Pachur, H.-J., Wünnemann, B., and Zhang, H. C. (1995). Lake evolution in the Tengger Desert, Northwestern China, during the last 40,000 years. *Quaternary Research* **44,** 171–180.

Peng, J. L., Zhang, H. C., and Ma, Y. Z. (1998). Late Pleistocene liminic ostracods and their environmental significance in the Tengger Desert, Northwest China. *Acta Micropalaeontologica Sinica* **15,** 22–30.

Porter, S. C., and An, Z. S. (1995). Correlation between climate events in the North Atlantic and China during the Last Glaciation. *Nature* **375,** 305–308.

Prell, W. L., and Kutzbach, J. E. (1987). Monsoon variability over the past 150,000 years. *Journal of Geophysical Research* **92,** 8411–8425.

Qi, Y. (1999). "The Character of Lacustrine Deposits and Climate Significance in Tengger Desert and Adjacent Regions since Late Pleistocene." Unpublished MSc thesis, Lanzhou University.

Rasmussen, T. L., Van Weering, T. C. E., and Labeyrie, L. (1997). Climatic instability, ice sheets and ocean dynamics at high northern latitudes during the last glacial period (58–10KA BP). *Quaternary Science Reviews* **16,** 71–80.

Ren, M. D., and Wang, N. L. (1980). "Modern Depositional Environments." Science Press, Beijing.

Rhodes, T. E., Gasse, F., Lin, R., Fontes, J.-Ch., Wei, K., Bertrand, P., Gibert, E., Melieres, F., Tucholka, P., Wang, Z., and Cheng, Z. (1996). A late Pleistocene-Holocene lacustrine record from Lake Manas, Zunggar (northern Xinjiang, western China). *Palaeogeography, Palaeoclimatology, Palaeoecology* **120,** 105–121.

Sirocko, F., Leuschner, D., Staubwasser, M., Maley, J., and Heusser, L. (1999). High-frequency oscillations of the last 70,000 years in the Tropical/Subtropical and Polar Climates. *In* "Mechanisms of Global Climate Variability at Millennial Timescales" (P. U., Clarke, R. S., Webb, and L. D. Keigwin, Eds.), pp. 243–262. *American Geophysical Union Monograph* **112**.

Thompson, L. G., Yao, T., Davis, M. E., Henderson, K. A., Mosley-Thompson, E., Lin, P.-N., Beer, J., Synal, H.-A., Cole-Dai, J., and Bolzan, J. F. (1997). Tropical climate instability: The last glacial cycle from a Qinghai-Tibetan ice core. *Science* **276,** 1821–1825.

Thomson, J., Higgs, N. C., and Clayton, T. (1995). A geochemical criterion for the recognition of Heinrich events and estimation of their depositional fluxes by the $(^{230}Th_{excess})_0$ profiling method. *Earth and Planetary Science Letters* **135,** 41–56.

Veiga-Pires, C. C., and Hillarie-Marcel, C. (1999). U and Th isotope constrains on the duration of Heinrich events H0-H4 in the southeastern Labrador Sea. *Paleoceanography* **14,** 187–199.

Wang, L. J., and Sarnthein, M. (1999). Millennial reoccurrence of century-scale abrupt events of East Asian monsoon: A possible heat conveyor for the global deglaciation. *Paleoceanography* **14,** 725–731.

Wünnemann, B., Pachur, H.-J., and Zhang, H. C. (1998). Climatic and environmental changes in the deserts of Inner Mongolia, China, since the Late Pleistocene. *In* "Quaternary Deserts and Climatic Changes" (A. S. Alsharhan, K. W. Glennie, G. L. Whittle, and C. G. St. C. Kendall, Eds.), pp. 381–394. Balkema, Rotterdaman.

Xiao, J. L., Porter, S. C., and An, Z. S. (1995). Grain size of quartz as an indicator of winter monsoon strength on the Loess Plateau of Central China during the last 130000 years. *Quaternary Research* **43,** 22–29.

Yao, T. D., Thompson, G. L., Shi, Y. F., Qi, D. H., Jiao, K. Q., Yang, Z. H., Tian, L. D., and Mosley-Thompson, E. (1997). Climatic change since last interglaciation in Gulia ice core. *Science in China* (series D) **27,** 447–452.

Zhang, H. C. (Ed.) (1997). "The Superficial Elemental Geochemistry and Theoretical Principles," (pp. 80–117). Lanzhou Univ. Press.

Zhang, H. C., and Wünnemann, B. (1997). Preliminary study on the chronology of lacustrine deposits and determination of high palaeolake levels in Tengger Desert since Late Pleistocene. *Journal of Lanzhou University* **33,** 87–91.

Zhang, H. C., Ma, Y. Z., Wünnemann, B., and Pachur, H.-J. (2000). A Holocene climatic record from arid Northwestern China. *Palaeogeography, Palaeoclimatology, Palaeoecology* **162,** 389–401.

Zhang, H. C., Li, J. J., Ma, Y. Z., Li, J. J., Qi, Y., Chen, G. J., and Fang H. B. (2001a). Late Paleolake Evolution and abrupt climate changes during Last *Glacial* period in NW China. *Geophysical Research Letters* **28,** 3203–3206.

Zhang, H. C., Li, J. J., Ma, Y. Z., Cao, J. X., Mu D. F., Chen, G. J., Fang H. B., Pachur, H.-J., and Wünnemann, B. (2001b). Late Quaternary palaeolake levels in Tengger Desert, NW China. *Palaeogeography, Palaeoclimatology, Palaeoecology* (in press).

Zhou, W. J., Donahue, D. J., Porter, S. C., Jule, T. A., Li, X. Q., Stuiver, M., An, Z. S., Eiji, M., and Dong, G. R. (1996). Variability of monsoon climate in East Asia at the end of the Last Glaciation. *Quaternary Research* **46,** 219–229.